COMPARISON OF TRANSIENT PCRV MODEL TEST RESULTS WITH ANALYSIS

A. H. MARCHERTAS
Argonne National Laboratory,
9700 South Cass Avenue, Argonne, Illinois 60439, U.S.A.

T. B. BELYTSCHKO
The Technological Institute,
Northwestern University, Evanston, Illinois 60201, U.S.A.

Summary

Comparisons are made of transient data derived from simple models of a reactor containment vessel with analytical solutions. This effort is a part of the ongoing process of development and testing of the DYNAPCON computer code.

The test results used in these comparisons were obtained from scaled models of the British sodium cooled fast breeder program. The test structure is a scaled model of a cylindrically shaped reactor containment vessel made of concrete. This concrete vessel is prestressed axially by holddown bolts spanning the top and bottom slabs along the cylindrical walls, and is also prestressed circumferentially by a number of cables wrapped around the vessel. For test purposes this containment vessel is partially filled with water, which comes in direct contact with the vessel walls. The explosive charge is immersed in the pool of water and is centrally suspended from the top of the vessel. The tests are very similar to the series of tests made for the COVA experimental program, but the vessel here is the prestressed concrete container.

The load history was obtained from an ICECO analysis, using the equations of state for the source and the water. A detailed check of this solution was made to assure that the derived loading did provide the correct input. The DYNAPCON code was then used for the analysis of the prestressed concrete containment model. This analysis required the simulation of prestressing and the response of the model to the applied transient load.

The calculations correctly predict the magnitudes of displacements of the PCRV model. In addition, the displacement time histories obtained from the calculations reproduce the general features of the experimented records: the period elongation and amplitude increase as compared to an elastic solution, and also the absence of permanent displacement. However, the period still underestimates the experiment, while the amplitude is generally somewhat large.

1. Introduction

Prestressed Concrete Reactor Vessels (PCRVs) may offer substantial advantages in LMFBR containment. The design and safety analysis of a PCRV, however, requires an analytical tool to predict the response of the containment under transient loading, particularly such as a hypothetical core disruptive accident. The code DYNAPCON was developed for the analysis of reinforced/prestressed structure under transient loading and is described in [1,2]. In this program a finite element method is used with explicit time integration, and a concrete model has been included to treat cracking and other characteristics of concrete behavior.

This paper describes the comparison of DYNAPCON results with a series of tests on 1/50 scale PCRV models. The code was able to predict the observed failure load, available displacement time histories and other salient features of the experiments. Thus, this comparison serves as a valuable preliminary step in the validation of this code.

2. Experimental Results

The data used in these comparisons were obtained from tests performed at Foulness 1/50 scale model of the prestressed concrete containment vessel for a sodium-cooled breeder, which were conducted for the British fast reactor safety program. A cross-section of this cylindrical PCRV model is shown in Fig. 1. It was loaded through charges submerged in the pool of water. The explosive used was the same PETN/polystyrene foam as in the COVA [3] test for which a well-defined equation of state exists. Most of the data pertain to one PCRV model within which a number of progressively larger charges were exploded. These tests were started with a charge of 2.5g (test 1), which produced no damage, and ended with the charge of 112g (test 7), which caused the concrete to be blown out through the sides of the vessel. A separate test was then made with the last charge on a completely new PCRV model. The results were similar to those of test 7.

Since the tests were not designed expressly for code validation, the usable amount of data for this purpose was quite limited. The available experimental data which pertains to the PCRV model is derived from tests 5 and 6. All tests possess a good collection of pressure readings enabling a rather detailed comparison with analysis concerning the PCRV loading. The properties of concrete and prestressing steel are given in Table I.

3. Analytical Approach

Because of the small size of the experimental vessel, only a few pressure transducers were included. Therefore, in order to obtain a set of consistent pressure records for use of the PCRV analysis, an ICECO [4] simulation of the charge detonation and subsequent pool swell and slug impact was made.

ICECO is an Eulerian implicit hydrodynamics code developed at Argonne. Although the program could be coupled with the structural PCRV program, the deformation of the PCRV model was too small to have any effect on the hydrodynamics. Therefore, the ICECO analysis was performed first with the PCRV walls assumed as rigid, and the resulting pressures were then used in the PCRV analysis. It should be pointed out that although the influence of the structure on the hydrodynamics is negligible, the fluid adjacent to the structure probably has a more pronounced effect on the structural response. However, because of the large number of runs required in these preliminary studies, coupled analyses were ruled out as too expensive.

3.1 ICECO Analysis

In the ICECO analysis, the behavior of the charge was described by the equation of state derived for the COVA experiments [3]:

$$p = Ae^{-9V} + Be^{-2.4V} + C^{-1.1} \tag{1}$$

where A = 17.039 GPa, B = 1.1595 GPa, C = 53.56 MPa, and V is the specific volume. The equation of state for water is of the form

$$p = \frac{B_o}{B'_o}\left[\left(\frac{V_o}{V}\right)^{B'_o} - 1\right] , \tag{2}$$

where B_o = 1.9895 GPa, B'_o = 6.985 GPa, and V_o is the initial specific volume. The air above the surface of the water was allowed to escape during the excursion and to present no resistance to compression.

A sequence of analytical ICECO pictures for test 8 at the specified times is given in Fig. 2. This shows the expansion of the source and the impact of fluid onto the top boundary. A set of corresponding pressure histories from test 8 are compared to the ICECO solutions in Fig. 3. The time scale of the experimental data was shifted to correspond with the analytical incident pressure. It is observed that the pressures at the base of the bottom slab agree for the initial pressure spike but deviate considerably in the subsequent pressure history. This large discrepancy is difficult to explain unless the pressure gauge during the second pressure rise can be dismissed as being faulty. This supposition is borne out by the results of test 7, where a similar source portrays a pressure trace like that shown by the analysis. This set of experimental data is shown in Fig. 4.

In general, the agreement at the side of the vessel for the initial pressure rise is quite good. The second pressure rise at about 1 ms is only shown by the experimental data. The peak of the incident pressure, however, is shown to agree with that of the first set of data. The third pressure rise, due to the reflective pressure caused by the impact of the fluid on the top surface, appears only in the analytical solution.

The peak pressure caused by slug impact given by the analysis is somewhat larger than that shown by the experiment, but the impulse of the incident pressure differs little. The shape of the roof pressure given in Fig. 4 seems to agree with the first set of data.

The impulse of the incident pressure of test and simulation compare favorably, but the subsequent pressure traces show more deviation. Of primary concern for the comparison are the loads at the side and the top of the tank, since those locations are critical in the PCRV model. Because the initial impulse of the pressure is reproduced reasonably well by analysis at the side and top of the vessel, it is concluded that the calculated pressure around the circumference can be used as the forcing function for the PCRV analysis.

Similar ICECO solutions were performed for all of the charges used in the experiments. The pressure histories on the walls of the PCRV were stored and used to load the prestressed PCRV analytical model.

3.2 PCRV Analysis

The PCRV model is shown in Fig. 5. Axisymmetric linear-displacement triangular elements with one integration point per element were used. Four layers of elements were used in the cylindrical walls, and although this is barely sufficient for an accurate simulation of the bending, the primary response is in a hoop mode, for which this discretization is more than adequate. The stable time step for this model was 2 μs, so 800 time steps were needed for

1.6 ms simulations.

The prestressing tendons were modelled by rod elements placed as shown in Fig. 5. An elastic-plastic material model with isotropic strain hardening was used for the rods. These elements were connected to the concrete elements through sliding interfaces, so that the prestressing force was applied to the PCRV only at the anchors of the tendons.

In the PCRV model the vertical tendons consisted of 18 high strength bolts of 12.7 mm diameter which were prestressed to an initial tension of 49 kN. Hoop prestress was applied by winding on the model 18 gauge (1.22 mm) diameter high tensile wire at tension of 1.46 kN. Due to the relaxation of the model, the estimated prestress in the tests were as follows [5]:

1. Hoop tendon loads were reduced 70% to 65% of their failure strength, and
2. Vertical tendon loads were reduced from 74% to 64% of their failure strength.

These estimated prestress conditions were used in our simulations; the equivalent values are indicated in Fig. 5.

The prestressing operation was simulated by applying equal and opposite forces to the concrete and prestressing members at the anchors with the tendons and concrete considered disconnected. A static solution was obtained for this condition by a dynamic relaxation procedure [2]. During the dynamic relaxation procedure, no cracking was allowed in the concrete to prevent spurious cracking from dynamic overshoots. The results of this solution then served as initial conditions for the transient solutions, except that the small residual velocities remaining from the relaxation procedure were eliminated to reduce noise in the transient solution.

4. Results

The response of the Foulness scale model was computed for each of the seven charges. Initially, we attempted to simulate the existing cracks in tests 4 to 7 by introducing the predicted cracks as initial conditions for subsequent simulations. However, we found the effect of cracks in the discrete model is more severe than in reality [2], so that the carryover of cracks resulted in premature failure. Therefore, all subsequent runs were made with either no initial cracks or at most precracking from one or two previous simulations.

The displacement history at the center wall for test 1 is shown in Fig. 6. This history first shows the effect of the pressure surge on the walls of the model, and later the response due to slug impact. In this simulation the stresses remain below the tensile limit and no cracking occurs. Table II gives experimental and analytical results of the maximum radial displacement for all of the seven tests, where no precracking had been assumed in the analytical simulation. The magnitude of the analytical results agrees well with those given by the experiment. For test 5, two values are given because the experimental results were not axisymmetric. In test 6, only one of the gauges worked. The analysis correctly predicts failure for the seventh charge. The correct prediction of failure required the incorporation of the strain rate dependence of concrete strength; without this, previous analysis also showed failure for a simulation of test 6.

Displacement histories at the midpoint of the cylindrical wall were available for test 5 and 6, so we will examine them in more detail. Figure 7 shows the experimental data of test 5, a simulation without precracking, a simulation with precracking resulting from the loading of test 4, and the simulation with accumulated precracking resulting from the loading of both test 3 and 4. The time of the analytical solution is shifted by 0.15 ms so that the initial deflection corresponds with that of the experimental data.

The computer simulations with cracking replicate the principal features of the experiment: the period of the displacement is increased, and the amplitude is increased as compared to the elastic solution. The precracked simulation is more accurate in the period, while that without precracking is more accurate in the maximum amplitude. Both solutions exhibit the absence of any permanent displacement found in the experiment: the prestressing tendons remain elastic and close the cracks after the load is released. Some of the disagreement between theory and experiment can be explained by the absence of the fluid in the model: its added mass would further elongate the period but reduce the amplitude. It is of interest that the solutions with and without precracking bound the observed maximum displacement.

The deformation history for test 6 is given in Fig. 8 where test data are compared to two analytical solutions. The analytical results consist of a purely elastic solution and another with cracking where precracking had not been taken into account. The correlation between the analytical predictions and experiment is almost identical to test 5: the amplitude agrees quite well, but the solution without precracking no longer bounds the observed displacement from below.

5. Conclusions

The results presented in this paper reflect the current capability of the DYNAPCON code to treat dynamically loaded PCRV structures. The comparisons of experiment and code results shows good agreement but also some areas of disagreement. The calculations correctly predict the failure of the PCRV model in test 7, and the magnitudes of the displacements for tests 5 and 6. In addition, displacement time histories obtained from the calculation reproduce the salient features of the experimental records: period elongation and amplitude increase as compared to an elastic solution, and the absence of permanent displacement. However, the period still underestimates the experiment, while the amplitude is generally somewhat large. In test 5, the solutions with and without precracking bound the observed record. Some of the discrepancy observed may be due to the absence of a fluid added mass in the computations.

One parameter in the transient modelling of concrete, which was introduced in this investigation, is the effect of strain rate on the tensile strength limit of concrete. The relevance of this parameter, although inferred only from intuition and numerical considerations, appears to be quite important in modelling of concrete cracking. Experimental evidence is necessary to resolve this issue. Once an experimental determination of the rate-dependence can be ascertained then the remaining questions of crack modelling can be addressed.

Although it is quite clear that analytical modelling of concrete cracking must include strain-rate effects, it is also evident that this is not the only cause for the disparity. This is indicated by the observation that analytical simulations could not quite match the experimental shapes of the deflections. Either the amplitude or the period of response could be varied by changing different variables, however, both of them could not be matched with experiment for the same run.

The need for experimental evidence into the phenomenology of concrete cracking cannot be overemphasized. Closer agreement with experimental data will eventually require better analytical modelling of the actual cracking phenomenon.

Acknowledgment

The experiemntal data used in this paper was provided to ANL by Mr. W. B. Dale, Fast Reactor Development, UKAEA. Mr. J. N. Bradbury of Nuclear Power Company (Risley) Limited provided additional information on the prestress relaxation of the test model. The actual testing was conducted at Foulness, where Mr. V. C. Pickett was the principal investigator.

The author acknowledges the council and help of Dr. S. H. Fistedis. Appreciation is also extended to the individual members of the Structural Mechanics Section for valued suggestions during the course of this study. This work was supported by the U. S. Department of Energy.

References

[1] MARCHERTAS, A. H., et al, "Analysis and Application of Prestressed Concrete Reactor Vessels for LMFBR Containment," Nucl. Eng. Design 49, pp. 155-173 (1978).

[2] MARCHERTAS, A. H., BELYTSCHKO, T., BAZANT, Z. P., "Transient Analysis of LMFBR Reinforced/Prestressed Concrete Containment," Trans. 5th Int. Conf. on SMiRT, Paper H 8/1, Berlin, (1979).

[3] CAMERON, I. G., HOSKIN, N. E., LANCEFIELD, M. J., "Charge Development and Analysis of Recent UK Experiments in the COVA Model Test Programme," Trans. of the 4th Int. Conf. on SMiRT, Paper E 2/1, San Francisco (August, 1977).

[4] WANG, CHUNG-YI, "ICECO - An Implicit Eulerian Method for Calculating Fluid Transients in Fast-Reactor Containment," Argonne National Laboratory Report, ANL-75-81, (December, 1975).

[5] Personal communication from J. N. Bradbury, Civil Department, Nuclear Power Company (Risley) Limited, Warrington Road, Risley, Warrington, Cheshire WA3 6BZ, England.

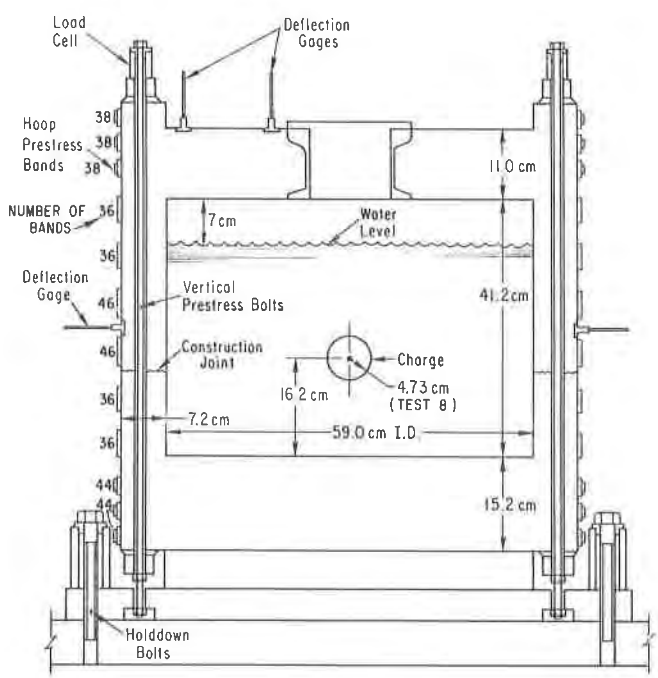

Fig. 1. Geometry of the Test Model.

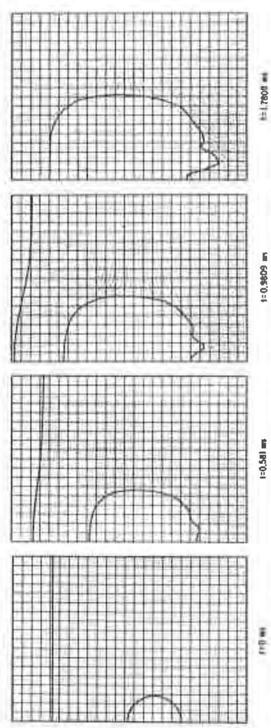

Fig. 2. Sequence of Analytical Configurations of the Excursion.

Table I. Material Properties

Properties of Concrete

Density	2400 kg/m^3
Modulus of elasticity	44000 MN/m^2
Stress-strain data (yield)	Tensile failure strength 5 MN/m^2 Compressive failure strength 60-70 MN/m^2
Poisson's ratio	0.17

Properties of Prestress Steel

Density	8000 kg/m^3
Initial modulus of elasticity	200000 MN/m^2
Tensile and compressive limits	Hoop prestress: 18 gage wire (1.22mm dia.) Tensile failure 2085N Vertical prestress: 12.7mm bolt Tensile yield load 66030N Tensile failure load 78680N
Poisson's ratio	0.30

Table II. Maximum Radial Displacement at the Side Wall

Test No.	Charge, g	Pressure*, MPa	Displacement, mm	
			Experiment	Analysis
1 & 2	2.5	3.6 & 2.5	-	0.103
3 & 4	14 & 12	6.8 & 15.9	-	0.343
5	27.	19.8	1.0, 0.77	0.871
6	54.	25.5	1.27	1.54
7	112.	44.0	Failure	-

*Recorded peak pressure on the side wall.

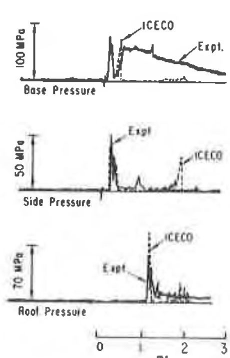

Fig. 3. Comparison of Analytical Solution with Experimental Results from Test 8.

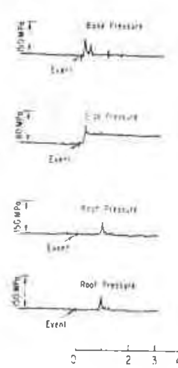

Fig. 4. Experimental Results from Test 7.

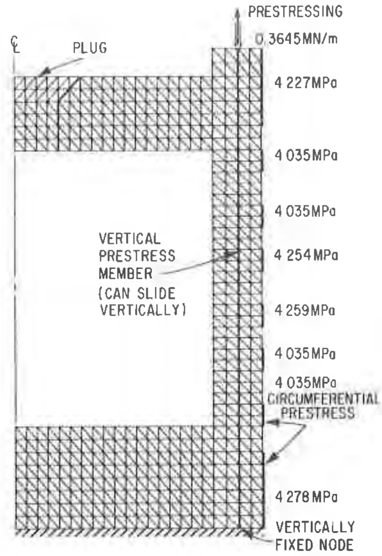

Fig. 5. The PCRV Analytical Model.

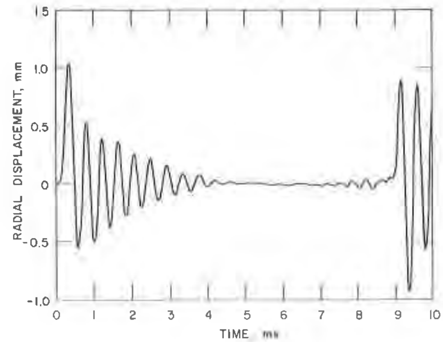

Fig. 6. Side Wall Displacement for Test 1.

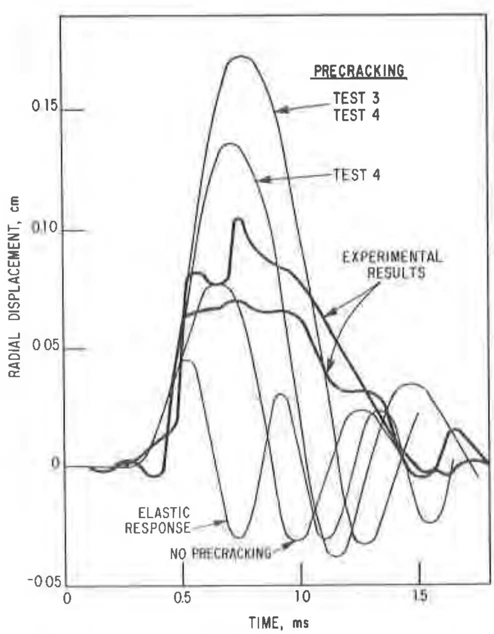

Fig. 7. Comparison of Side Wall Displacement for Test 5.

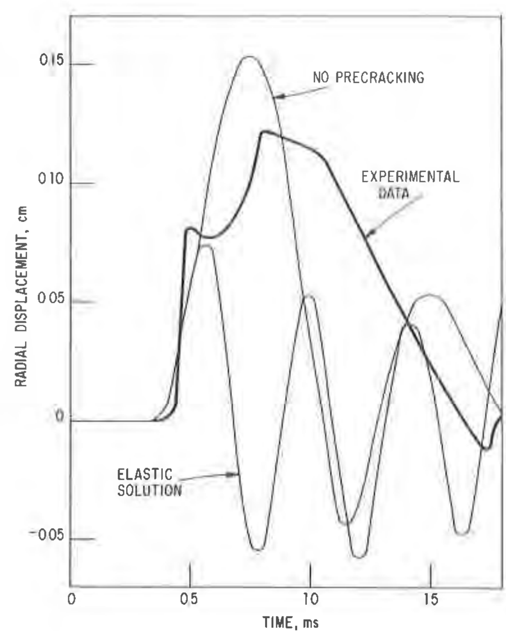

Fig. 8. Comparison of Side Wall Displacement for Test 6.